



Magnetocaloric response of amorphous and nanocrystalline Cr-containing Vitroperm-type alloys

L.M. Moreno-Ramírez¹, J.S. Blázquez¹, V. Franco¹, A. Conde¹, M. Marsilius², V. Budinsky², G. Herzer²

¹Dpto. Física de la Materia Condensada, ICMSE-CSIC, Universidad de Sevilla, P.O. Box 1065, 41080-Sevilla, Spain

²Vacuumschmelze GmbH & Co KG, Grüner Weg 37, D-63450 Hanau, Germany

Abstract

The broad compositional range in which transition metal (TM) based amorphous alloys can be obtained, yields an easily tunable magnetocaloric effect (MCE) in a wide temperature range. In some TM-based alloys, anomalous behaviors are reported, as a non-monotonous trend with magnetic moment (e.g. FeZrB alloys). Moreover, in certain Cr-containing Vitroperm alloys anomalously high values of the magnetic entropy change were published. In this work, a systematic study on MCE response of Cr-containing amorphous alloys of composition $\text{Fe}_{74-x}\text{Cr}_x\text{Cu}_1\text{Nb}_3\text{Si}_{15.5}\text{B}_{6.5}$ (with $x=2, 8, 10, 12, 13, 14$ and 20) has been performed in a broad Curie temperature range from 100 K to 550 K. Curie temperature and magnetic entropy change peak of the amorphous alloys decrease with the increase of Cr content at rates of -25.6 K/at.% Cr and -54 mJkg⁻¹K⁻¹/at.% Cr, respectively, following a linear trend with the magnetic moment in both cases. The presence of nanocrystalline phases has been considered as a possible cause in order to explain the anomalies. The samples were nanocrystallized in different stages, however, the magnetocaloric response decreases as crystallization progresses due to the large separation of the Curie temperatures of the two phases.

Introduction

Magnetic refrigeration is called to be an energetic efficient green alternative to the usual refrigeration systems based on the compression-expansion of gasses. Magnetic refrigeration is based on the magnetocaloric effect (MCE), defined as the temperature change under a magnetic field variation in an adiabatic process (ΔT_{ad}) or as the magnetic entropy change in an isothermal process due to a magnetic field variation (ΔS_M) [1]. From Maxwell relations ΔS_M can be expressed as: $\Delta S_M = \mu_0 \int_0^H \left(\frac{\partial M}{\partial T} \right)_H dH$, where M , T , H and μ_0 are the magnetization, temperature, magnetic field and magnetic permeability of vacuum, respectively. From that, it is deduced that the MCE is maximum around a phase transition which implies magnetization changes, either with first (FOPT) or second order (SOPT) character. FOPT materials show high magnetocaloric peaks but in a narrow temperature range. Moreover, they normally present associated hysteresis phenomena. On the other hand, SOPT materials show smaller magnetocaloric peaks but in a wider temperature range than FOPT materials and without associated hysteresis. In this sense, transition metal (TM) based amorphous alloys have been widely studied since they were proposed as low cost candidates for magnetocaloric applications due to the easily tuned Curie temperature (T_C), negligible magnetic hysteresis, high electrical resistivity (decreasing eddy current losses) and excellent mechanical properties [2-5]. In addition to this potential for applications, they constitute model systems in which detailed studies of the different magnitudes affecting magnetocaloric response could be analyzed, like scaling of the properties [6], influence of demagnetizing field [7] or interphase interactions [8], etc.

The MCE response of Cr-containing amorphous alloys has been reported with extremely high ΔS_M^{peak} values [9]. However, these values are not in agreement with

other data found in the literature [10-12]. These anomalies could be due to a non-monotonous behavior of the magnetic moment with the addition of different elements in the amorphous matrix (as it has been found for FeZrB alloys [13]) or to a composite character of the system [14]. In this work, a systematic study on the MCE response of a Cr-containing amorphous alloy series has been performed. This series extends in a very broad Curie temperature range, from $\sim 100\text{K}$ to 550 K . The possible causes of the described anomalies are explored.

Experimental

Ribbon samples of composition $\text{Fe}_{74-x}\text{Cr}_x\text{Cu}_1\text{Nb}_3\text{Si}_{15.5}\text{B}_{6.5}$ (with $x=2, 8, 10, 12, 13, 14$ and 20) were produced by melt spinning. Throughout the paper, samples are referenced by its Cr content. Microstructural characterization of the samples was done by x-ray diffraction (XRD) experiments with $\text{Cu K}\alpha$ radiation in a Bruker D8I diffractometer. The study of the thermal stability and the heat treatments of the samples was performed by differential scanning calorimetry (DSC) in a Perkin–Elmer DSC7 under Ar flow. Magnetic measurements were performed in a Lakeshore 7407 vibrating sample magnetometer (VSM) equipped with a cryostat down to 77.7 K or an oven up to 1300 K . Samples with $\sim 25\ \mu\text{m}$ of thickness were cut as discs of 3 mm diameter to minimize the effect of the demagnetizing factor and sample positioning. The mass of the samples was measured in a Mettler Toledo XP26 scale with an accuracy of $1\ \mu\text{g}$. Magnetocaloric analysis has been performed using the software Magnetocaloric Effect Analysis Program [15], available from LakeShore Cryotronics Inc.

Results

Figure 1 shows the XRD patterns of the as-quenched Cr-containing Vitroperm ribbons in which it can be observed that samples are fully amorphous, independently of the Cr

content. Concerning the thermal stability, figure 2 shows the DSC scans of the as-quenched amorphous ribbons. From these scans up to 993 K at 20 K/min, two transformation processes can be observed, although the high temperature one shifts out of the explored range as the Cr content decreases. The first process corresponds to the crystallization of the bcc-Fe nanophase (α -Fe), as confirmed by XRD experiments (figure 7). The increase of Cr content shifts the nanocrystallization peak to higher temperatures, stabilizing the amorphous structure. For the sample with 20 at.% Cr, the primary crystallization peak overlaps with high temperature processes and the nanocrystalline state is not observed.

Magnetic entropy change curves were calculated using the software previously mentioned using a numerical approximation to the Maxwell equation. Figure 3 shows the specific magnetization, $\sigma(T)$, at 200 Oe (upper panel) and $\Delta S_M(T)$ for a magnetic field change of 15 kOe (lower panel) for the amorphous ribbons. From $\sigma(T)$ data it can be observed that the Curie temperature of the amorphous alloys decreases as Cr content increases. This variation follows a linear dependence with a slope of -25.6 ± 0.8 K/at.% of Cr, in agreement with previous studies [16]. Although the increase in Cr content allows us to reduce T_C , it is at the expense of a decrease of the magnetic entropy change peak (ΔS_M^{peak}) (figure 4). The refrigerant capacity (RC), calculated as the product of ΔS_M^{peak} times the full width half maximum (FWHM), also decreases with the increase of Cr content, although the variation is less significant than for ΔS_M^{peak} (comparing samples with 2 and 14 at.% of Cr, the variation of the ΔS_M^{peak} is about 56%, meanwhile, for RC it is 18%). For the sample with 20 at.% Cr, RC cannot be calculated because the FWHM is out of the cryostat range. Both variations of ΔS_M^{peak} and RC are explained by the reduction of magnetic moment with the increase of Cr content in Vitroperm alloys following a dilution law [17,18], as can be observed in inset of figure 5. In fact, a linear

evolution between ΔS_M^{peak} and the magnetic moment in Fe atoms (μ_{Fe}) can be observed (figure 5). The magnetocaloric response of the studied amorphous ribbons have been compared to other previously studied amorphous series including bulk amorphous [19-21], Vitroperm [10-12,22,23] and Nanoperm [2,24-45] compositions, as it is shown in figure 6. Values from literature were rescaled to 10 kOe using a power law with $n=0.75$ [46]. The values obtained in this study for the samples containing Cr are in agreement with those Vitroperm type alloys without anomalous response [10-12].

Although the anomalous high values were assigned for amorphous samples, in order to explore a suitable cause for anomalies in MCE response the presence of small amount of nanocrystals have been considered. The samples were nanocrystallized to produce composite materials. The thermal treatments were performed in the differential scanning calorimeter at two stages of the first transition process, T1 and T2, corresponding to the mid-point temperature between the onset and the peak temperatures and to the peak temperature, respectively (figure 2). With respect to the microstructural characterization, crystal size (D) and crystalline fraction (X_C) were obtained from XRD experiments (figure 7). D was estimated using the Scherrer formula and X_C was obtained from the area ratio between the amorphous halo and the (110) α -Fe line. The deconvolution of amorphous halo and crystalline peak has been done using Gaussian and Lorentzian peaks, respectively (figure 8). For both heat treatments, the crystalline fraction is reduced and the crystal size increases as Cr content increases in the alloy. Combining these two facts it is deduced that Cr hinders the nucleation of the α -Fe nanocrystals in the amorphous matrix. With respect to the magnetocaloric response, figure 9 shows ΔS_M for samples nanocrystallized with 2 and 14 at.% Cr along with the response of the corresponding amorphous alloy for comparison. The magnetocaloric response clearly decreases as the crystallization fraction increases which is due to the

high Curie temperature of the crystalline phase with respect to that of the amorphous phase, reducing the amount of phase that has a significant MCE response at the studied temperature. Therefore nanocrystallization cannot explain the extremely high ΔS_M values reported earlier for Cr-containing alloys (6). Thus these previous results appear to be due experimental artifacts still to be clarified. It can also be observed that crystallization of α -Fe phase changes the composition of the residual amorphous matrix, varying its Curie temperature. This fact explains why the high temperature response of the samples is not monotonous with the crystalline fraction. Changing the temperature axis (used in figure 9) to a reduced temperature axis, $t=(T-T_C)/T_C$, the expected monotonous behavior with the increase in crystalline fraction is recovered (insets of figure 9).

The magnetic entropy change can be expressed as a power law of the form $\Delta S_M=aH^n$, where n is field independent for single phase materials in three regimes: well below T_C ($n=1$), well above T_C ($n=2$) and at T_C (related with the critical exponents of the transition) [46]. TM-based amorphous alloys shows similar values of exponent n at T_C around 0.75, as it is observed in our amorphous samples. Figure 10 shows, as an example, $n(T)$ curves for the amorphous and nanocrystalline samples with 2 at.% Cr. The influence of the crystalline phase (ferromagnetic α -Fe impurities) in the nanocrystallized samples can be observed in the departure of the exponent n at T_C and above T_C from the predicted values for single phase materials. Inset of figure 10 shows the evolution of the exponent $n(T_C)$ with the crystalline fraction obtained from XRD experiments, in which n departs to higher values than that typically found in amorphous alloys (~ 0.75). Above T_C , the influence of the ferromagnetic α -Fe ($n=1$) phase does not allow to achieve the expected value for the paramagnetic phase ($n=2$).

Conclusions

In this work, the influence of the Cr content on the magnetocaloric response of amorphous Vitroperm-type ribbons is studied. The increase in Cr content reduces T_C at a rate of -25.6 ± 0.8 K/at.% Cr, as well as the magnetic entropy change peak, at a rate of -54 mJkg⁻¹K⁻¹/at.% Cr. This reduction of the magnetocaloric response is related to the decrease of the magnetic moment as Cr content increases. The obtained values are in agreement with the general trend observed for TM-based amorphous alloys and a reduction of T_C is observed at the expense of a decrease of the MCE response. It has been found that the nanocrystallization of the samples deteriorates the magnetocaloric response due to the large difference between the Curie temperatures of the crystalline and amorphous phases.

Acknowledgements

This work was supported by the Spanish MINECO (project MAT2013-45165-P) and the PAI of the Regional Government of Andalucía. L.M. Moreno-Ramírez acknowledges a FPU fellowship from the Spanish MECD.

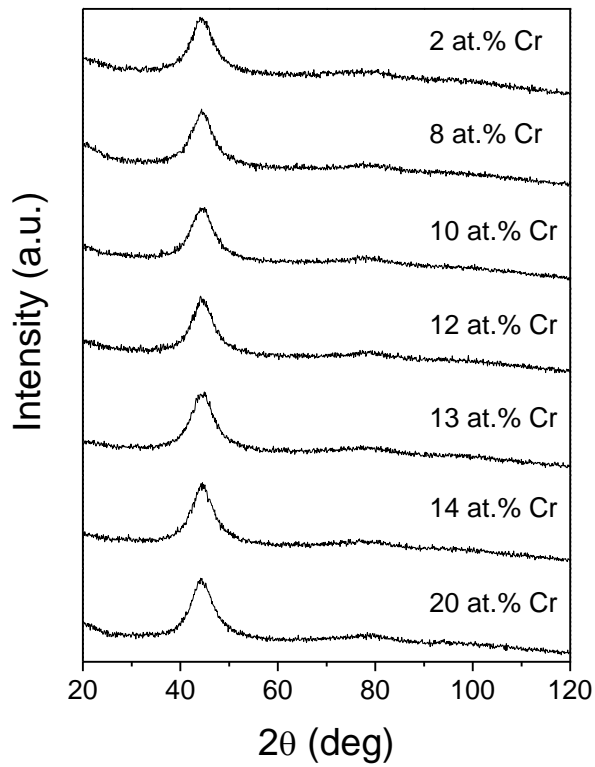


Figure 1. XRD patterns of the as-quenched Cr-containing Vitroperm alloys.

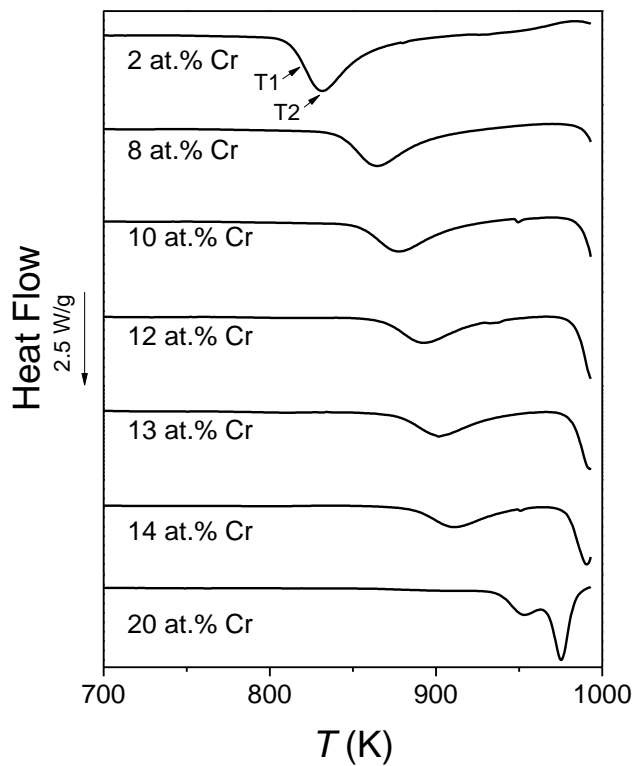


Figure 2. DSC scans of the as-quenched Cr-containing Vitroperm alloys.

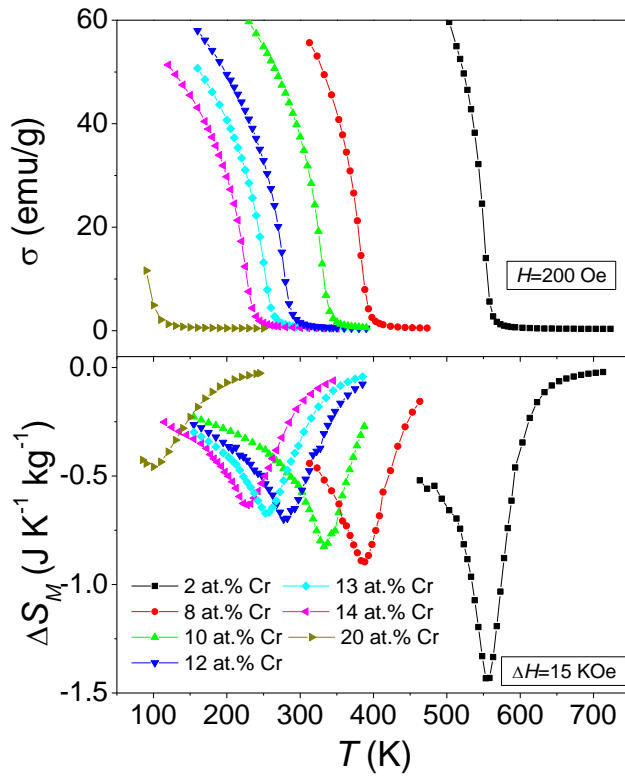


Figure 3. Specific magnetization (σ) at 200 Oe (upper panel) and magnetic entropy change (ΔS_M) up to 15 kOe (lower panel) for the amorphous ribbons.

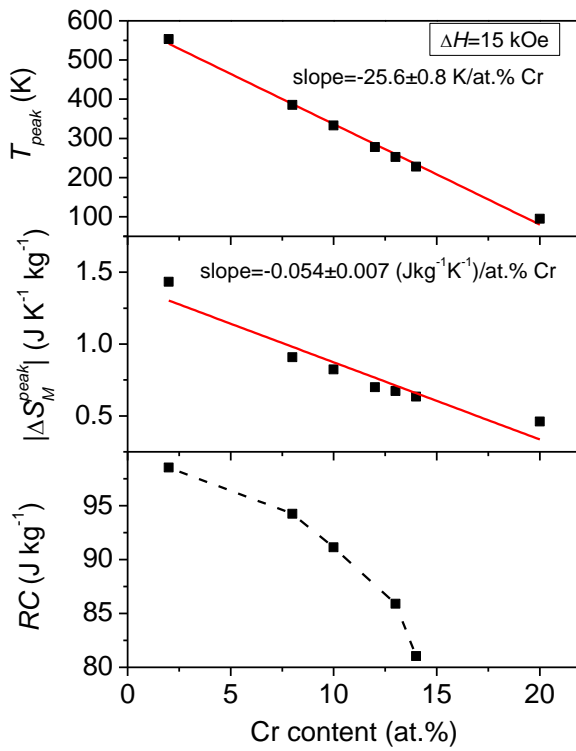


Figure 4. Peak temperature of ΔS_M (T_{peak}), Maximum $|\Delta S_M|$ and refrigerant capacity (RC) vs nominal Cr content of the amorphous ribbons.

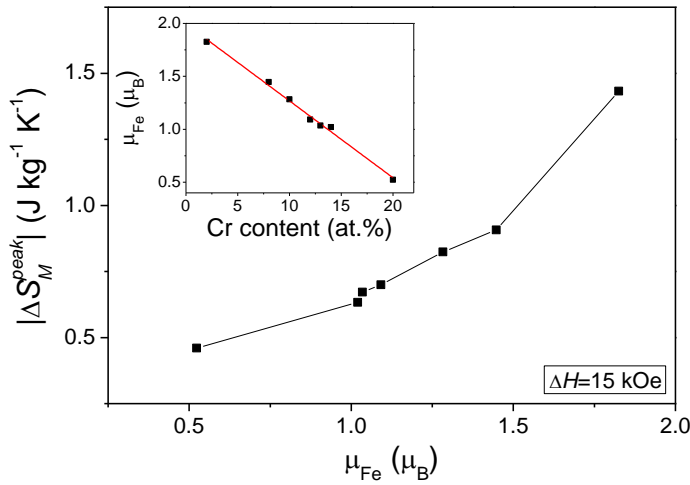


Figure 5. Magnetic entropy change peak (ΔS_M^{peak}) vs magnetic moment per Fe atom (μ_{Fe}) in amorphous alloys. Inset: μ_{Fe} as a function of Cr content from [17].

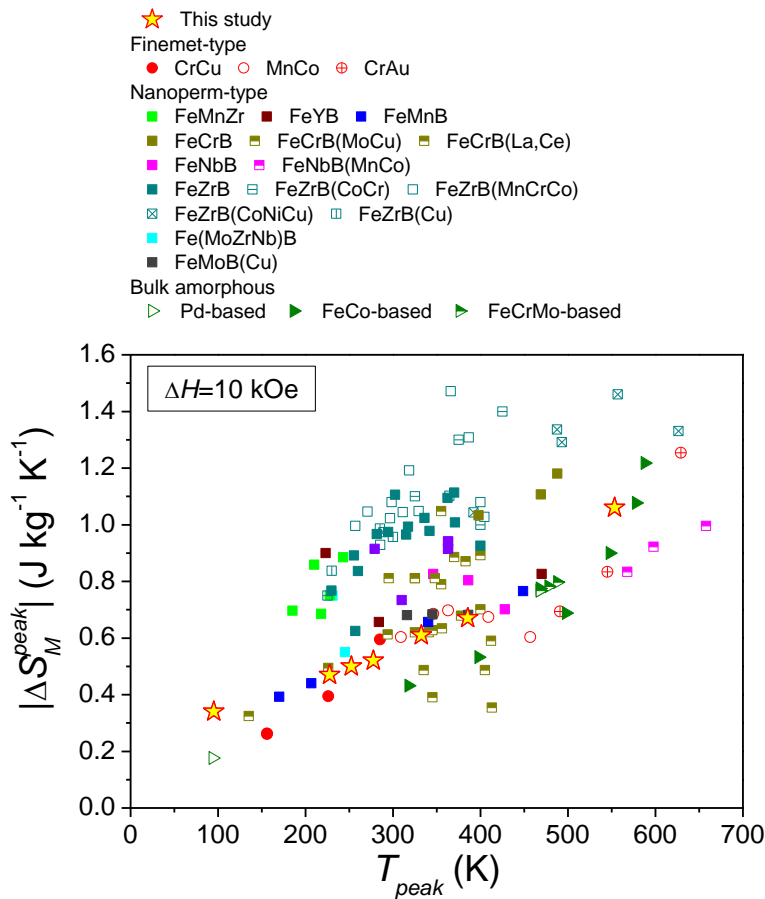


Figure 6. Magnetic entropy change peak (ΔS_M^{peak}) vs peak temperature (T_{peak}) at 10 kOe for different transition metal based amorphous alloys [2,10-12,19-45].

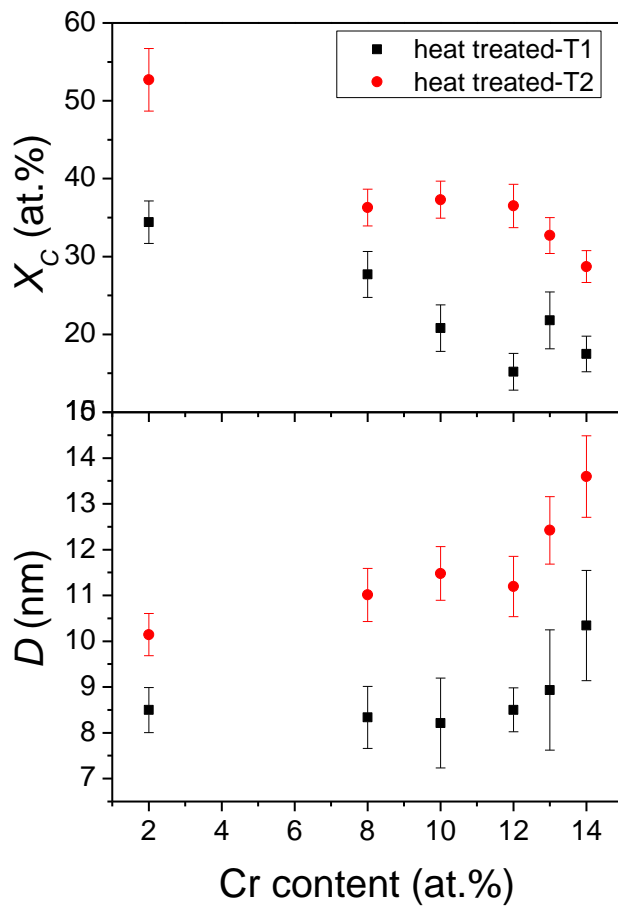


Figure 7. Crystalline fraction (X_C) and crystal size (D) obtained from XRD experiments.

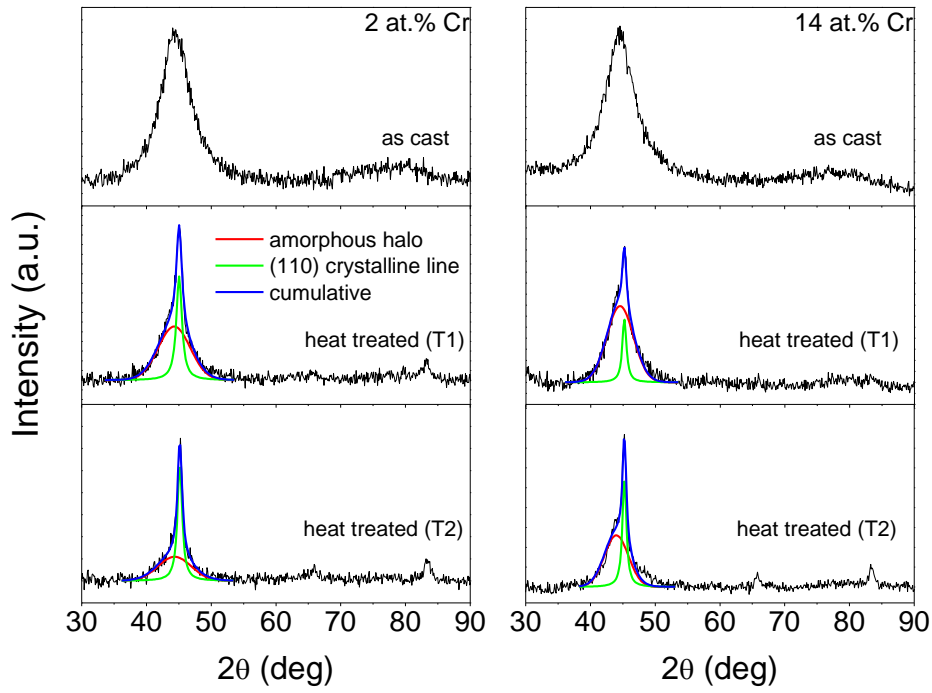


Figure 8. XRD patterns of 2 and 14 at.% of Cr samples after heat treatments. Deconvolutions of amorphous halo and (110) crystalline line are shown.

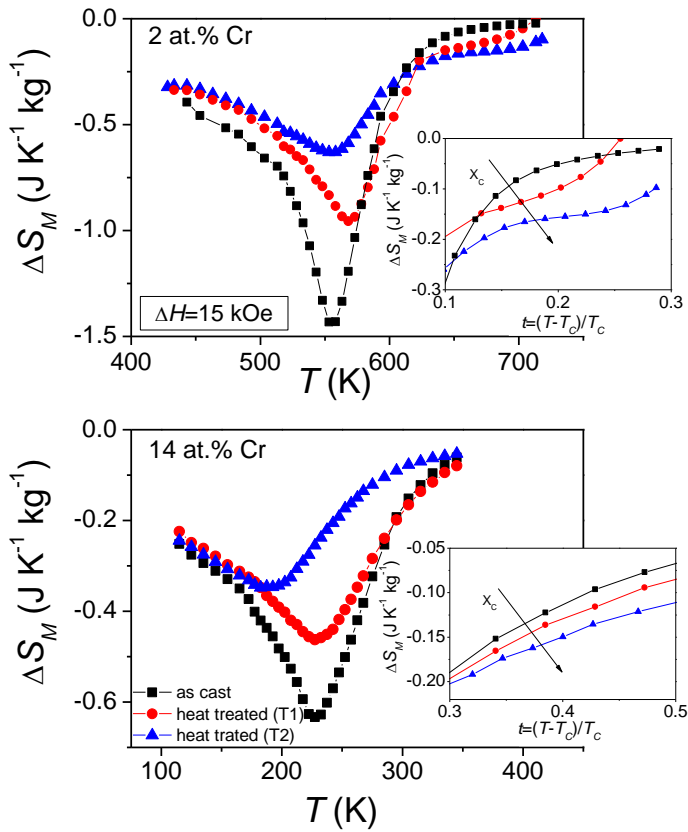


Figure 9. Evolution of ΔS_M with crystalline fraction for 2 and 14 at.% Cr samples. Inset: high temperature response vs reduced temperature (t).

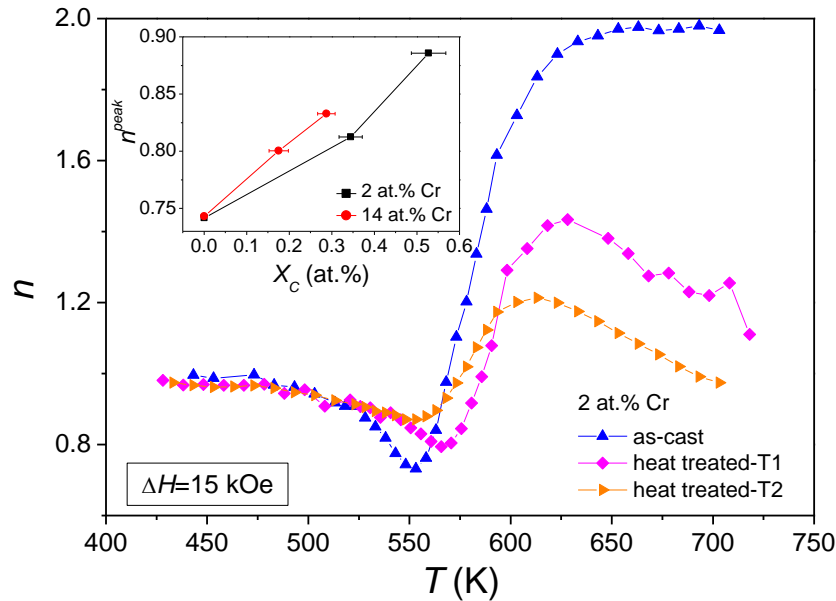


Figure 10. Exponent n for the as-cast and heat treated samples with 2 at.% Cr. Inset: Evolution of the exponent n^{peak} with X_C (XRD experiments).

References

- [1] V. Franco, J.S. Blázquez, B. Ingale, A. Conde, *Annu. Rev. Mater. Res.* 42 (2012) 305.
- [2] I. Skorvanek and J. Kovac, *Czech. J. Phys.* 54 (2004) D189
- [3] F. Johnson and R. D. Shull, *J. Appl. Phys.* 99 (2006) 08K909
- [4] V. Franco, J.S. Blázquez, C.F. Conde, A. Conde, *Appl. Phys. Lett.* 88 (2006) 042505.
- [5] V. Franco, A. Conde, *Scripta Materialia* 67 (2012) 594.
- [6] V. Franco, A. Conde, J.M. Romero Enrique, J.S. Blázquez, *J. Phys.: Condens. Matter* 20 (2008) 285207.
- [7] L.M. Moreno-Ramírez, J.J. Ipus, V. Franco, J.S. Blázquez, A. Conde, *J. All. Compd.* 622 (2015) 606.
- [8] C. Romero-Muñiz, V. Franco, A. Conde, *Appl. Phys. Lett.* 102 (2013) 082402.
- [9] N. Chau, P.Q. Thanh, N.Q. Hoa, N.D. The, *J. Magn. Magn. Mater.* 304 (2006) 36.
- [10] V.S. Kolat, S. Atalay, *Magnetocaloric behaviour in Fe₅₇Cr₁₇Cu₁Nb₃Si₁₃B₉ soft magnetic alloys*, Weinheim: Wiley-VCH Verlag GmbH; 2004.
- [11] S. Atalay, H. Gencer, V.S. Kolat, *J. Non-Cryst. Solids* 351 (2005) 2373.
- [12] A. Kolano-Burian, M. Kowalczyk, R. Kolano, R. Szymczak, H. Szymczak, M. Polak, *J. All. Compd.* 479 (2009) 71.
- [13] L. F. Kiss, T. Kemény, V. Franco, A. Conde, *J. All. Compd.* 622 (2015) 756.
- [14] R. Caballero-Flores, V. Franco, A. Conde, K.E. Knipling, M.A. Willard, *Appl. Phys. Lett.* 98 (2011) 102505.
- [15] <http://www.lakeshore.com/products/Vibrating-Sample-Magnetometer/Pages/MCE.aspx>.
- [16] V. Franco, C. Conde, A. Conde, B. Varga, A. Lovas, *J. Magn. Magn. Mater.* 215-216 (2000) 404.

- [17] M.A. Hakim, S. M. Hoque, S.S. Sikder, Md.S. Mahmud, P. Norblad, J. Korean. Phys. Soc. 53 (2008) 766.
- [18] K. Inomata, M. Hasegawa, S. Shimanuki, S. Sahashi, J. Magn. Soc. Jpn. 5 (1981) 57.
- [19] T.D. Shen, R.B. Schwarz, J.Y. Coulter, J. Appl. Phys. 91 (2002) 5240.
- [20] V. Franco, J.M. Borrego, A. Conde, S. Roth, Appl. Phys. Lett. 88 (2006) 132509.
- [21] V. Franco, J.M. Borrego, C.F. Conde, A. Conde, M. Stoica, S. Roth, J. Appl. Phys. 100 (2006) 083903.
- [22] J. H. Lee, S.J. Lee, W.B. Han, H.H. An, C.S. Yoon, J. All. Compd. 509 (2011) 7764.
- [23] S.G. Min, L.G. Ligay, K.S. Kim, S.C. Yu, N.D. Tho, N. Chau, J. Magn. Magn. Mater. 300 (2006) E385-E7.
- [24] D.H. Wang, K. Peng, B.X. Gu, Z.D. Han, S.L. Tang, W. Qin, et al. J. All. Compd. 358 (2003) 312.
- [25] J. Torrens-Serra, P. Bruna, S. Roth, J. Rodriguez-Viejo, M.T. Clavaguera-Mora, J. Phys. D-Appl. Phys. 42 (2009) 095010.
- [26] I. Skorvanek, J. Kovac, J. Marcin, P. Svec, D. Janickovic, Mat. Sci. Eng. A-Struc. Mat. Prop. Micr. Proc. 449 (2007) 460.
- [27] J. Kovac, P. Svec, I. Skorvanek, Rev. Adv. Mater. Sci. 18 (2008) 533.
- [28] S.G. Min, K.S. Kim, S.C. Yu, H.S. Suh, S.W. Lee, J. Appl. Phys. 97 (2005) 10M310.
- [29] S.G. Min, K.S. Kim, S.C. Yu, Y.C. Kim, K.Y. Kim, K.W. Lee, et al. J. Magn. Magn. Mater. 310 (2007) 2820.
- [30] V. Franco, J.S. Blázquez, A. Conde, J. Appl. Phys. 100 (2006) 064307.
- [31] V. Franco, C.F. Conde, J.S. Blázquez, A. Conde, P. Svec, D. Janickovic, et al. J. Appl. Phys. 101 (2007) 093903.
- [32] V. Franco, C.F. Conde, J.S. Blázquez, M. Millan, A. Conde, J. Appl. Phys. 102 (2007) 013908.
- [33] V. Franco, C.F. Conde, A. Conde, L.F. Kiss, Appl. Phys. Lett. 90 (2007) 052509.
- [34] V. Franco, A. Conde, L.F. Kiss, J. Appl. Phys. 104 (2008) 033903.
- [35] R. Caballero-Flores, V. Franco, A. Conde, K.E. Knipling, M.A. Willard, Appl. Phys. Lett. 96 (2010) 182506.
- [36] J.Y. Law, V. Franco, R.V. Ramanujan, J. Appl. Phys. 110 (2011) 023907.
- [37] J.Y. Law, V. Franco, R.V. Ramanujan, Appl. Phys. Lett. 98 (2011) 192503.
- [38] F. Johnson, R.D. Shull, J. Appl. Phys. 99 (2006) 08909.
- [39] K.S. Kim, S.G. Min, S.C. Yu, S.K. Oh, Y.C. Kim, K.Y. Kim, J. Magn. Magn. Mat. 304 (2006) E642-E4.
- [40] Y.K. Fang, C.C. Yeh, C.C. Hsieh, C.W. Chang, H.W. Chang, W.C. Chang, et al. J. Appl. Phys. 105 (2009) 07A704.
- [41] Y.Y. Wang, X.F. Bi, Appl. Phys. Lett. 95 (2009) 262501.
- [42] P. Alvarez, J.S. Marcos, P. Gorria, L.F. Barquin, J.A. Blanco, J. All. Compd. 504 (2010) S150-S4.
- [43] P. Alvarez, J.L.S. Llamazares, P. Gorria, J.A. Blanco, Appl. Phys. Lett. 99 (2011) 232501.
- [44] J. Swierczek, T. Mydlarz, J. All. Compd. 509 (2011) 9340.
- [45] D. Mishra, M. Gurram, A. Reddy, A. Perumal, P. Saravanan, A. Srinivasan, Mat. Sci. Eng. B-Adv. Func. Solid-State Mat. 175 (2010) 253.
- [46] V. Franco, J.S. Blázquez, A. Conde, Appl. Phys. Lett. 89 (2006) 222512.